Biogeosciences Discuss., 10, 3849–3889, 2013
www.biogeosciences-discuss.net/10/3849/2013/
doi:10.5194/bgd-10-3849-2013

Biogeosciences Discussions Open Access

Ocean Colour remote sensing in the Southern Laptev Sea: evaluation and applications

B. Heim[1], E. Abramova[5,6], R. Doerffer[2], F. Günther[1], J. Hölemann[1,6], A. Kraberg[1], H. Lantuit[1], A. Loginova[3,4,6], F. Martynov[4,6], P. P. Overduin[1], and C. Wegner[3]

[1]Alfred-Wegener-Institut Helmholtz-Zentrum für Polar- und Meeresforschung, Germany
[2]Helmholtz Centre Geesthacht HZG, Institute for Coastal Research, Geesthacht, Germany
[3]GEOMAR Helmholtz Centre for Ocean Research, Kiel, Germany
[4]St. Petersburg University, St. Petersburg, Russia
[5]Lena Tiksi Reservate, Russia
[6]Otto Schmidt Laboratory OSL, St. Petersburg, Russia

Received: 21 December 2012 – Accepted: 21 January 2013 – Published: 28 February 2013

Correspondence to: B. Heim (birgit.heim@awi.de)

Published by Copernicus Publications on behalf of the European Geosciences Union.

Abstract

Enhanced permafrost warming and increased arctic river discharges have heightened concern about the input of terrigeneous matter into Arctic coastal waters. We used optical operational satellite data from the Ocean Colour sensor MERIS onboard the ENVISAT satellite mission for synoptic monitoring of the pathways of terrigeneous matter in the southern Laptev Sea. MERIS satellite data from 2006 on to 2011 were processed using the Case2Regional Processor, C2R, installed in the open-source software ESA BEAM-VISAT.

Since optical remote sensing using Ocean Colour satellite data has seen little application in Siberian Arctic coastal and shelf waters, we assess the applicability of the calculated MERIS parameters with surface water sampling data from the Russian-German ship expeditions LENA2010 and TRANSDRIFT-XVII taking place in August and September 2010 in the southern Laptev Sea. The surface waters of the southern Laptev Sea are characterized by low transparencies, due to turbid river water input, terrestrial input by coastal erosion, resuspension events and, therefore, high background concentrations of Suspended Particulate Matter, SPM, and coloured Dissolved Organic Matter, cDOM.

The mapped calculated optical water parameters, such as the first attenuation depth, Z_{90}, the attenuation coefficient, k, and Suspended Particulate Matter, SPM, visualize resuspension events that occur in shallow coastal and shelf waters indicating vertical mixing events. The mapped optical water parameters also visualize that the hydrography of the Laptev Sea is dominated by frontal meanders with amplitudes up to 30 km and eddies and filaments with diameters up to 100 km that prevail throughout the ice-free season. The meander crests, filaments and eddy-like structures that become visible through the mapped MERIS C2R parameters indicate enhanced vertical and horizontal transport energy for the transport of terrigenous and living biological matter in the surface waters during the ice-free season.

1 Introduction

The aim of this study is to apply Ocean Colour remote sensing to gather information on the hydrodynamics in the Laptev Sea, Siberian Arctic. Ocean Colour remote sensing uses optical satellite data from Ocean Colour satellite missions and applies Ocean Colour algorithms for Case-1 and Case-2 surface waters: useful operational Ocean Colour remote sensing products are optical parameters such as attenuation and absorption, and optically visible water constituents, such as chlorophyll (Chl *a*), Suspended Particulate Matter (SPM), and coloured Dissolved Organic Matter (cDOM). The 3rd report (2000) of the International Ocean Colour Coordinating Group (IOCCG, http://www.ioccg.org/) described the phenomenon of optically complex surface waters (coastal waters, fluvial and limnic systems) designating such surface waters as Case-2 waters in contrast to Case-1 waters dominated optically by phytoplankton with coupled organic and particulate matter concentrations from autochthonous production. In general, in Case-2 surface waters the phytoplankton does not vary proportionally with other optically visible constituents, because cDOM and particles originate from allochthonous sources (Morel and Prieur, 1977; Lee and Hu, 2006). The Ocean Colour processing linked to Case-2 waters requires sophisticated atmospheric correction schemes due to non-zero upwelling radiances in the NIR wavelength region and sophisticated bio-optical algorithms to account for cDOM and particulates in particular.

Optical remote sensing applications in polar regions are also limited by the prevailing low solar elevations, and the persistence of clouds and fog (International Ocean Colour Coordinating Group (IOCCG), http://www.ioccg.org/). Since 2010, the COAST-Colour project (http://www.coastcolour.org/) of the European space Agency, ESA, has incorporated the Kara Sea and Laptev Sea regions into its program for evaluating the applicability of Ocean Colour remote sensing in Arctic coastal waters. For the Laptev Sea, the Ocean Colour remote sensing analyses are carried out within the framework of this study and Örek et al. (2013).

Within this study, the optical remote sensing parameters were calculated from optical Medium Resolution Imaging Spectrometer (MERIS) data. MERIS is the Ocean Colour sensor on board the ENVIronment SATellite (ENVISAT), an ESA satellite mission that could operate until early 2012. We used the Regional Case2 (C2R) Processor Module (developed by Doerffer and Schiller, 2007, 2008), Brockmann Consult (DE), in cooperation with the Norwegian Institute for Water Research and the Canadian Institute of Ocean Sciences) installed in the open source software BEAM-VISAT (Brockmann Consult) provided by ESA. C2R processes the MERIS Top-Of-Atmosphere (TOA) radiances to water leaving reflectances, and calculated optical coefficients and concentrations of optically visible water constituents (Chl *a*, SPM, cDOM).

We evaluated the applicability of the optical parameters calculated from the MERIS satellite data by investigating the ranges of concentrations of optically visible parameters from field-based sampling and by comparing the field-based data with the remote sensing-derived data. Field-based useful parameters are turbidity, transmissivity, SPM, cDOM, and phytoplankton via its optical proxy Chl *a*.

Since ship-based sampling is logistically constrained in spatial and temporal coverage, optical satellite data provide additional data in space and time, visualising the hydrodynamical spatial structures. By examining the spatial pattern of Ocean Colour parameters, we hope to gain insights from optically visible events towards information on surface water processes in the sea ice-free season.

2 Hydrography of the Laptev Sea

The Laptev Sea is an open marginal sea of the Arctic Ocean bounded by the Taimyr Peninsula on the west and the New Siberian Islands on the east (Fig. 1a). Together with the Eastern Siberian shelf the Laptev Sea region is part of the world's broadest shelf system. Atmospheric forcing, sea ice dynamics, freshwater river input and terrestrial fluxes from the coastal zone strongly influence the shallow shelf waters and their biogeochemistry. Sea-ice processes affect the early freshwater runoff, the erosion of

coastal cliffs and the erosion of shallow submarine tectonic horsts and islands. Sediments scraped up from shallows and suspended particulate matter from the water column are incorporated and transported via the sea ice (Aagaard and Armack, 1989; Eicken et al., 1997; Wegner et al., 2005).

The Siberian river systems deliver large volumes of freshwater and dissolved and particulate matter into the Arctic Siberian Shelf system (Gordeev et al., 1996; Rachold et al., 2000; Lobbes et al., 2000). The Lena River is the second largest Arctic river and discharges 581 km^3 freshwater annually (Holmes et al., 2012), delivering an average annual sediment input of 20.7 $Mt\,yr^{-1}$ (Rachold et al., 2004). Most of the water is discharged during end of May and beginning of June when the ice in the rivers breaks up but the Laptev Sea is still covered by sea-ice (Holmes et al., 2012). The Lena River Delta is the largest Arctic delta and undergoes considerable block uplift that controls the delta's topography and drainage system (Fig. 1b). The main modern Lena river branches enter the Buor Khaya Gulf through the northern and eastern part of the Lena River Delta: the Sardakhsko-Trofimovskaya channel systems with 60–75 % of the Lena River water discharge, and the Bykovskaya channel up to 25 % of water discharge (Charkin et al., 2011). The Olenyeksky and Tumatskaya branches with up to 10 % of water discharge flow westwards, emptying southwards of the western Lena River Delta into the Laptev Sea (in Charkin et al., 2011). Elevated Pleistocene terraces without an active drainage system build up the north-western part of the Lena River Delta.

Large parts of the Central and Eastern Siberian coastline are characterized by the highly erosive sedimentary ice-rich Yedoma (Ice-Complex) (Lantuit et al., 2011, 2012). The Ice Complex is a pleistocene stratigraphic unit composed of very ice-rich (usually > 80 % by volume) organic-rich deposits (Schirrmeister et al., 2002). The delivery of terrestrial and dissolved organic material from this permafrost coastal zone considerably contributes to the carbon pool in Arctic coastal waters (e.g. Charkin et al., 2011; Vonk et al., 2011, 2012; Rachold et al., 2004). Karlsson et al. (2011), Sánchez-García et al. (2011) and Vonk et al. (2012) discuss the input of terrigeneous Particulate Organic Matter (POC) with old POC originating from Yedoma, the younger to modern

POC originating from the fluvial discharges. Terrestrial markers such as lignin, and other markers are present over the Siberian shelf area (Vonk et al., 2012; Gustavson et al., 2011; Lobbes et al., 2000) proving a large-scale spatial distribution of terrestrial matter.

All described processes deliver large volumes of organic-rich terrestrial matter in particulate and dissolved form into the Laptev Sea shelf system.

3 Material and methods

3.1 Surface water sampling and analyses

In August 2008, the Russian–German ship expedition LENA08 sampled water along the coast of the Bykovsky Peninsula Ice Complex in the western Buor Khaya Bay (Fig. 1a, b) (Wagner et al., 2012). In summer 2010, from 29 July to 8 August 2010, the Russian–German LENA10 ship expedition sampled in the Buor Khaya Bay (Figs. 1a, b, 2 and Appendix I, Table 1a). The Russian–German ship expedition TRANSDRIFT-XVII took place in September 2010 from 9 to 20 September 2010 (Kassens et al., 2010) (Figs. 1a, 3 and Appendix I, Table 1b).

On the LENA2010 and the TRANSDRIFT-XVII expeditions hydrographical investigations were carried out with Conductivity, Temperature, Depth meter (CTD) sensor casts with a Sea and Sun Technology GmbH (USA) on the LENA2010 expedition, and a SeaBird Electronics (USA) SBE19+ connected to a carousel water sampler SBE32C on the TRANSDRIFT-XVII expedition. The CTD SBE19+ was equipped with additional sensors for measuring water turbidity (Seapoint OBS), dissolved oxygen concentration and Chl *a* fluorescence (WETlabs WETstar, USA). A second CTD cast was operated with a WETstar CDOM sensor (WETlabs, USA). According to previous work the WETlabs in-situ Chl *a* fluorescence ($mg\,m^{-3}$) shows an overestimation of a factor of 3.5 compared to in-situ Chl *a* by direct sampling and is accordingly corrected by this factor.

The water samples were filtered and prepared at site. 0.5 L was filtered for SPM through 0.45 µm pore size MILLIPORE Durapore membrane filters, for Chl *a* through 0.7 µm pore size Whatman GF filters with a pressure of not more than 0.2 bar. One litre was filtered through 0.45 µm-pore size preweighed cellulose-acetate (CA) filters for SPM and through 0.7 µm-pore size glass-fibre (GF) filters for DOC and cDOM. The Chl *a* filters were immediately frozen on site. cDOM filtrates were stored in brown quartz glass bottles and kept cooled and in the dark.

cDOM was measured immediately following each expedition at the Russian–German Otto-Schmidt Laboratory (OSL) in St. Petersburg using a Specord200 (Jena Analytik). Optical Density (OD) spectra of the filtrates were measured from 300 nm to 750 nm in 1 nm steps using 5 cm and 10 cm cuvettes, according to the absorption capacity of the samples (Scott et al., 2000). Absorption per m was calculated using 2.303× OD/0.1 for the 10 cm-cuvette, and 2.303× OD/0.05 for the 5 cm-cuvette, respectively. Chl *a* from the filters was measured at the OSL in St. Petersburg (RU) using a TD-700 fluorimeter.

3.2 Satellite data processing and analyses

Ocean Colour remote sensing uses spectro-radiometrically highly-performing optical satellite sensors (http://www.ioccg.org/). The two Moderate Resolution Imaging Spectroradiometer (MODIS) missions on the platforms TERRA and AQUA are currently operating Ocean Colour missions (http://modis.gsfc.nasa.gov/). MERIS was operated on ESA's ENVISAT from 2002 to early 2012 as a wide field-of-view imaging spectrometer with a swath width of 1150 km. MERIS measured the solar radiation reflected by the Earth's surface in the visible (VIS) and near infrared (NIR) wavelength ranges in fifteen spectral bands from 390 nm to 1040 nm.

MERIS Reduced Resolution (RR) is approximately 1 km at nadir (1040 m × 1200 m pixel) and available with a global daily coverage until 2012. We found for the time window of the sea-ice free season from 2006 to 2011 in the months of July, August, September between five and fifteen MERIS acquisitions per year that show relatively large cloud-free areas of the Laptev Sea region. MERIS-RR Level 1B TOA radiances

were processed using BEAM-VISAT4.9© with the MERIS Case-2 Regional Processor for coastal application (C2R; Doerffer and Schiller, 2007, 2008). The C2R processing modules use neural networks to inversely model water leaving reflectances of MERIS spectral bands 1–8 from calculated TOA reflectances after ozone, water vapour and surface pressure correction. Inverse modelling using neural networks is then used to derive aquatic parameters from the water leaving reflectances. The bio-optical forward model is parameterized with spectro-radiometric coefficients specific to coastal Case-2 waters (Doerffer and Schiller, 2007, 2008). The C2R processing modules are continuously updated and optimized (http://www.brockmann-consult.de/cms/web/BEAM/software).

C2R output parameters are estimated atmospheric and aquatic parameters, such as the water-leaving radiances and reflectances, the attenuation, absorption and backscattering coefficients, and calculated concentrations of Chl *a* (C2R_Chl *a*), Total Suspended Matter, TSM (C2R_TSM) equalling SPM, and gelbstoff absorption (C2R_a_gelbstoff) equalling cDOM. The three optical components calculated for the MERIS band 2 (central wavelength at 443 nm): absorption of phytoplankton pigments (C2R_a_pig); scattering of all particles b_tsm, (C2R_TSM); and absorption of dissolved organic material (C2R_a_gelbstoff) form the basis for calculating the concentrations. Chl *a* concentration is determined from an empirically derived relationship between absorption (a_pig) and Chl *a* concentration, and the dry weight of TSM from its empirically derived relationship with b_tsm, equals the operational parameter SPM with $mg\,L^{-1}$ a_gelbstoff, absorption of gelbstoff at 442.5 nm equals cDOM absorption (Doerffer and Schiller, 2007, 2008).

The properties of Beer's Law describe that each dimensionless unit of optical depth corresponds exponentially to a reduction of the intensity to e^{-1} or ∼ 37 % of its initial value. The vertical attenuation of sun light with depth can be described by the exponential equation, where the coefficient k is called the attenuation coefficient and is measured in m^{-1}. C2R_k_{min}, the diffuse coefficient of the minimum attenuation, is calculated within the Photosynthetically Active Radiation, PAR, wavelength region. All the

calculated remote sensing optical parameters and concentrations are representative for the first attenuation depth that is equivalent to the water depth layer wherefrom 90 % of the water leaving signal originates, Z_{90}. It is the depth at which the surface light field reduces to e^{-1} or ∼ 37 % of its initial value. The C2R parameter of the first attenuation depth, C2R_Z90, is calculated according to the two-flow model from Gordon and McCluney (1975) by:

$$Z_{90}(\lambda) = \frac{2.3}{2K_{\mathrm{d}}(\lambda)}, \quad \mathrm{m} \tag{1}$$

The euphotic depth, Z_{Eu}, down to which significant phytoplankton photosynthesis can occur, is set to the depth where the incident surface light falls to 1 % of that just below the surface. Z_{Eu} is not a C2R-processed parameter but can be calculated from the remote sensing C2R_k_{min} as:

$$Z_{\mathrm{Eu}}(\lambda) = \frac{4.6}{K(\lambda)}, \quad \mathrm{m} \tag{2}$$

For the Laptev Sea region, a problem is undetected thin cloud coverage and thin fogs that cannot be detected within the automatic processing. These artefacts are visible in the atmospherically processed Level-2 products as highly sharply-outlined features with under-and overestimated magnitudes of parameters. In the current state, these areas are manually excluded according to their sharply-outlined features before matching them with field-based data. There is the choice of raising the cloud-detection threshold level for the TOA radiances. However, coastal turbid waters would be excluded using higher thresholds for TOA radiances. Investigations are on-going to automatically correct for thin cloud coverage and thin fog covers. The Figs. 2, 3, 8 and 9 display the mapped C2R parameters with the background of the Google EarthTM land mosaic and the IBCAO bathymetry (©2010 Google, Image©2012 TerraMetrics, Image IBCAO) with the land and detected clouds transparently masked.

4 Results

4.1 Ranges of optically visible water parameters in the Southern Laptev Sea

The investigated near shore and offshore water types in the Buor Khaya Bay were characterized by low transparencies. Lena river waters had high turbidity, with in-situ Secchi depths of less than 0.5 m. Onshore waters in the Buor Khaya Bay (up to 2 to ∼ 5 m water depth) showed in-situ Secchi depth transparencies of 1 to 1.5 m in 2008, and measured transmissivity ranging from 60 to 75 % in 2010. Offshore waters (> 8 m water depth) had in-situ Secchi depth transparencies of up to 2 m in 2008. In 2010, the sampling covered a much larger region that included also transparent surface waters.

Measured cDOM values in Lena river waters and in the surface waters of the Buor Khaya Bay of the LENA2008 and LENA2010 expeditions were of high magnitudes in 2008 and 2010. Ranges for the absorption of cDOM at 443 nm, $a443_{\mathrm{cDOM}}$, were: Lena River, $a443_{\mathrm{cDOM}}$: 1.3–3.5 m^{-1}; mixed onshore waters, $a443_{\mathrm{cDOM}}$: 2.5–4 m^{-1}; offshore waters (stratified waters, > 8 m water depth), $a443_{\mathrm{cDOM}}$: 2–3 m^{-1}, coastal waters close to meltwater outflows of the permafrost-coast showed considerable highest $a443_{\mathrm{cDOM}}$ values: 3–7 m^{-1}.

The TRANSDRIFT-XVII samples also show elevated surface water cDOM concentrations in onshore and offshore inner shelf waters. Because the spectro-photometrically measured cDOM covered more sampling stations, the data analyses presented in this paper used the spectrophotometrical cDOM data. The spectrophotometrically measured cDOM absorption correlated also well with the in-situ cDOM fluorescence (Quinine Sulphate Dihydrate units) measured with WETSTAR (R^2 = 0.94), demonstrating the instrument's good performance in the waters of the Laptev Sea. The cDOM results, both spectrometrically measured and by fluorescence, showed a nearly conservative mixing within a wide salinity range (0–32). The range of cDOM concentrations of the TRANSDRIFT-XVII transect going northwards through the Buor Khaya Bay were $a443_{\mathrm{cDOM}}$ 2.2 m^{-1} and 1.5 m^{-1} for samples 1 to 3 and 5 to 6, respectively. More than

100 km north of the Lena River Delta along the east-west transect, high cDOM concentrations of $a443_{cDOM} = 1.2\,m^{-1}$ were still encountered (samples 8–17). The mid-shelf to outer-shelf transects had background concentrations of $a443_{cDOM} = 0.6\,m^{-1}$. Northwestward to the Taymir Peninsula $a443_{cDOM}$ was $0.4\,m^{-1}$. A $a443_{cDOM}$ maximum of $1.7\,m^{-1}$ occurred north of the New Siberian Islands (sample 19).

In summary, cDOM background concentrations were high, also in the surface water layer of the stratified off-shore waters and connected to the freshwater signal. The cDOM concentration of the Lena River in August 2008, and August 2010 was of the same magnitude as the cDOM concentrations of the coastal waters that surrounded the eastern Lena River Delta and the cDOM concentrations in Buor Khaya Bay in August 2008, August 2010, and September 2010.

On the mid- and outer shelf surface waters vary between 0.5 and $1\,mg\,L^{-1}$. TRANSDRIFT-XVII SPM ranges in 2010 showed concentrations from 1.5 to $2\,mg\,L^{-1}$ in Buor Khaya Bay (samples 1–3) with peaks of SPM concentrations within the first 2 m water layer of 5 to $6\,mg\,L^{-1}$ further north (samples 4, 10, 16). Wegner et al. (2013) describe the spatial variability of surface SPM distribution on the Laptev Sea shelf between years from multi-year TRANSDRIFT expedition data. Within the turbid surface water layer the SPM concentrations varied between $1\,mg\,L^{-1}$ at the front between the river-dominated and shelf waters and up to $18\,mg\,L^{-1}$ near the Lena Delta.

Investigations on phytoplankton (filter and in-situ fluorescence-derived Chl *a*) of multi-year TRANSDRIFT expedition data report always medium Chl *a* concentrations in surface waters from onshore to offshore waters. In 2010, the concentrations of TRANSDRIFT-XVII Chl *a* were from $1.9\,\mu g\,L^{-1}$ to $2.5\,\mu g\,L^{-1}$ Chl *a* in the Buor Khaya Bay (samples 1–3) and strongly connected to the freshwater signal. The thickness of the layer was about 12 m with a temperature of 7.8 °C and a salinity (Practical Salinity Unit, PSU) of 6 to 9. The east-west transect north of the Lena River Delta (samples 8–17) showed transitional hydrological values with temperatures around 3 °C, an averaged salinity of 22.6 and about $1\,\mu g\,L^{-1}$ Chl *a* at the stations. An exceptional high Chl *a* concentration occurred at station 12 (128° E, 74.20° N) with a maximum value of

$8\,\mu g\,L^{-1}$. In deeper shelf waters Chl *a* concentrations of the surface layer varied around $0.5\,\mu g\,L^{-1}$ Chl *a*. An area of elevated Chl *a* concentrations in surface waters of the outer shelf had concentrations of 1.5 to $2\,\mu g\,L^{-1}$ Chl *a* (samples 30–34) in marine waters of 32 salinity.

4.2 Evaluation of MERIS C2R parameters

The MERIS acquisitions on 31 July, 3–6 August and 10 August 2010 show low cloud coverage and are close in time to the LENA2010 ship expedition in Buor Khaya Bay that took place from 29 July to 7 August 2010. A MERIS acquisition on 7 September 2010 is the cloud-free acquisition closest in time to the TRANSDRIFT-XVII expedition that took part from 9–20 September 2010. The next usable MERIS acquisitions on 18 and 20 September 2010, have higher cloud coverage.

The in-situ data taken for the evaluation of the MERIS C2R parameters are averaged over the first 2 m water layer for transmissivity, cDOM, SPM and Chl *a*. CTD data from the LENA2010 and the TRANSDRIFT-XVII expedition show a homogenous, mixed layer covering this depth: stratification due to the riverine freshwater occurred in the Buor Khaya Bay with a sharp halocline below 5 to 8 m in August 2010 during the LENA2010 expedition (Kraberg et al., 2013), and below 10 m in September 2010 during the Buor Khaya transect and the east-west transect north of the Lena River Delta of TRANSDRIFT-XVII (Kassens et al., 2010).

Exact match-up analyses take the remote sensing value from the pixel location on the same day of the ship-based in-situ measurement. For the Laptev Sea region this is not feasible due to frequent cloud coverage. Match-up analyses using spatial averages of pixels could be a technical solution. However, for the Laptev Sea, the high-spatial and high-temporal horizontal heterogeneity confounds the spatially averaged match-up analyses. The analyses of matching pairs of cloud-free pixels and the LENA2010 expedition data cover a range of values of the optical parameters connected to turbidity within the Buor Khaya Bay, but no types of highly transparent waters. The matching of

pairs of cloud-free pixels and TRANSDRIFT-XVII expedition data cover a larger variety of optical surface water types including transparent water types of the outer shelf.

Figure 2a–c show the high spatial- and temporal variability of MERIS C2R_Z90 on 3, 4, 5 August 2010. For example, the LENA2010 sampling stations 1 to 3 and 25 are of the turbid water-type with values of C2R_Z90 ∼ 1 m on 3 August 2010, changing to more transparency with values of C2R_Z90 ∼ 2 m only within 1 to 2 days due to frontal changes.

The best matching coordinate pairs in time from the LENA2010 expedition (Table 1) and the TRANSDRIFT-XVII expedition (table 2) were selected for the match-up analyses. The match-up analyses using SPM data show a well-developed relationship between the optical C2R parameters connected to suspended matter (e.g. C2R_k_{min}, C2R_b_tsm (scattering of TSM), C2R_Z90, C2R_TSM) although there is a temporal difference of 2 to 11 days between the in-situ sampling and the MERIS acquisition on 7 September 2010.

Figure 4a shows the relationship TRANSDRIFT-XVII SPM versus C2R_ Z90 (7 September 2010), and Fig. 5 the relationship TRANSDRIFT-XVII SPM versus C2R_TSM (7 September 2010). The match-up analyses based on LENA2010 in-situ data in the Buor Khaya Bay showed the limits of relating to concomitant pixels of C2R parameters in optically highly heterogeneous and dynamic coastal waters.

The match-up analyses for cDOM and SPM versus C2R_kmin and C2R_Z90 show for near-coast on-shore waters that the major direct relationship exists between transmissivity and SPM. This optimal relationship (e.g. Fig. 4a, C2R_Z90 versus SPM) indicates that the turbidity/particulate matter is the dominating Ocean Colour producing aquatic component in the water-leaving spectral reflectances. The relationship C2R_Z90 versus cDOM (e.g. Fig. 4b) shows that cDOM influences the transparency parameters (C2R_kmin, C2R_Z90), but is not as dominating as SPM (Fig. 4a).

The derived concentration parameter C2R_Chl *a* processed with the standard BEAM VISAT C2R Chl *a* conversion factor = 21 from C2R_a_pig are overestimated by an order of magnitude. In general, calculated C2R_Chl *a* concentrations in Buor Khaya Bay

during the ice-free season show up to 20 to 30 µg L^{-1} C2R_Chl *a* for all the years 2006 to 2011. Chl *a* overestimation by the order of one magnitude is also characteristic to the global standard NASA SeaWiFS and MODIS Chl *a* products. As an example, we also included the match-ups of the MODIS Level3 binned Chl *a* averaged product for September 2010 (9 km spatial pixel resolution) versus the TRANSDRIFT-XVII Chl *a* data (Fig. 6). Figure 7 indicates how the magnitude of cDOM concentration correspondingly influences the calculated values of MERIS C2R_Chl *a*.

4.3 Spatio-temporal Ocean Colour synoptic information

The spatial distribution of different water types in the southern Laptev Sea can be visualized using the mapped MERIS C2R-parameters. For the Laptev Sea region, the temporal resolution of usable MERIS satellite data time series lies between daily resolution (in case of low cloud coverage) to monthly (in case of high cloud coverage, as is common during the ice-free season). The mapped optical parameters and concentration parameters provide information on the hydrodynamical meso-scale structures, such as meanders with amplitudes of 20 to 30 km and of filaments and eddies with diameters up to 100 km (e.g. Figs. 2, 3, 9). Filaments of the turbid water type with low transparencies (low C2R_Z90, high C2R_k_{min}) and high SPM (high C2R_TSM) frequently developed within Buor Khaya Bay. MERIS C2R-time series show that the filaments may be cut off the front and travel through the southern part of Buor Khaya Bay. The temporal resolution of all these spatially well-defined features is very high between one or few days. During this time span, filaments and meanders may change abruptly (e.g. Fig. 2). Figure 8 shows the mapped calculated MERIS C2R-parameters C2R_TSM (mg L^{-1}), C2R_Z90 (m), and C2R_ absorption (m^{-1}), of a cloud-free MERIS acquisition on Sep 25, 2009. High absorption is wide-spread in the Southern Laptev Sea. Intense meandering between turbid waters and less turbid waters is predominately found around the Lena River Delta and in zones of shallow banks and regions. The range of MERIS C2R_TSM range (2006 to 2010) in turbid regions shows concentrations from 5

to 12 mg L^{-1} and Z_{Eu} from C2R_Z90 of maximal 5 m. Calculated Z_{Eu} ranges outside the turbid water zones in the off-shore surface waters of Buor Khaya Bay showed values down to a 10 m euphotic water layer. In August 2010, an irregularly-shaped, transparent eddy system showed up in central Buor Khaya Bay (Fig. 2) with C2R_ZEu values of 13 m of the euphotic depth layer.

High turbidity is regularly visible on the shallow banks around the Lena River Delta and in the vicinity around the New Siberian Islands. The mapped C2R-parameters indicate that frequently, the turbidity zones considerably enlarge along the coastlines and also occur above shallow banks. The turbidity zones suggest that considerable remobilization of sea surface sediments due to resuspension events occur on the Laptev Sea and the Eastern Siberian shallow shelfs.

We also investigated if the outline of the Lena River freshwater plume is visible in the mapped MERIS C2R-parameters expecting to detect high SPM, high attenuation and absorption and low transparencies. Unfortunately, the event of the spring freshet is mostly hidden for optical remote sensing applications under the continuous cloud coverage in the months of June and early July. From 2006 to 2011, only very few acquisitions in early summer, 1 July 2009, and 3 July 2011, capture the spring freshet. Örek et al. (2013) describe the Lena River outflow during the spring freshet into the surrounding ice-free waters in early July. During the spring freshet, elevated parameters of SPM, absorption and attenuation and low transparencies with the spatial outline of a plume are visible only in the case of no low-ice coverage, such is the case in 2011, but not in 2009 with sea ice.

From mid of July until the end of September in all investigated years, the Lena River fresh water plume is not outlined and detectable as a spatially-outlined plume structure. Instead, on the wide shallow bench around the Lena River delta and on the shallow banks directly north-east of the Lena River Delta, elevated SPM-related C2R-parameters are regularly visible (Figs. 2, 3, 8). Northeast of the Lena River Delta at the outlets of the Lena River branches, regularly, meanders and filaments, sometimes of

a dipole type (with meander crests and filaments developing in more than one direction), are developing and being pushed outwards.

The LENA2010 expedition data show that a strong stratification with a mixed layer with a 5 to 8 m depth existed in Buor Khaya Bay in the beginning of August 2010. The on-shore transects (stations 15 to 18) occurred on 1 August 2010 within the fully mixed layer of high turbidity. At the LENA2010 expedition, the turbidity zone in coastal waters above the shallow Lena River Delta banks incorporated both, freshwater surface stations (< 1 salinity) and freshwater-influenced stations (< 5 salinity). Stations with below-brackwater salinities (< 5 salinity) can be found within all ranges of turbidity. This indicates that the Lena River freshwater signal (< 5 salinity) is not directly linked to elevated SPM-related C2R parameters in coastal waters. The riverine turbidity of the Lena River is optically hidden in the turbidity of coastal waters influenced by resuspension above the shallow Lena River Delta bench. The eastern Buor Khaya coast delivered fluvial discharge (e.g. station 8, < 1 PSU). A brackish surface water layer (> 8 PSU) of surface waters occurred outside the Buor Khaya Bay (stations 6, 7, 24; Fig. 2).

The MERIS acquisitions in early August 2010 (e.g. Figs. 2, 9a) show transparent coastal waters along the eastern coastline of Buor Khaya Bay indicating no intense resuspension within this coastal region of steeper submarine slopes. Therefore, on 8 August 2010, mapped C2R parameters could visualize ta turbid river inflow into the non-turbid coastal waters of eastern Buor Khaya Bay (Fig. 9a). However, after several storm events (http://www.ncep.noaa.gov/) in the southern Laptev Sea region in August and September 2010, we assume that the mixed upper layer became deeper and went down to a depth of at least 10 to 12 m in September 2010, as it was measured on the TRANSDRIFT XVII expedition. We can see that the MERIS acquisition on 27 August 2010, makes resuspension visible along all of the eastern coastline of the Buor Khaya Bay (Fig. 9b) and the turbid river inflows can no more be distinguished from the turbid coastal waters. The high spatial resolution extracted from the Rapid-Eye satellite data (5 m per pixel at nadir) on 8 and 27 August 2010, confirm the hydrodynamic interpretation of the coarser-scale MERIS satellite data for the more shallow mixed layer in

early August and on the deeper vertical mixing and resuspension events late in August (Fig. 9a, b).

5 Discussion

5.1 Evaluation of MERIS C2R parameters

The evaluation suggests that due to highly dynamic hydrography in the Southern Laptev Sea region, match-up analyses are difficult. Exact match-up analyses (that the remote sensing value is exactly taken from the pixel location on the same day of the ship-based in-situ measurement) seem mostly not to be feasible due to frequent cloud coverage and the high-spatial and high-temporal horizontal heterogeneity of the surface mixed layer. Also, match-up analyses using averages of pixels would be misleading along frontal zones. Therefore, we used the cloud-free pixels most closely in time that was feasible for match-ups based on the LENA2010 expedition data in early August 2010 and with a temporal difference of more than one week for the match-up analyses based on the TRANSDRIFT2010 expedition data.

Optical C2R parameters such as C2R Z90 and concentration parameters such as C2R TSM could be reasonably used to trace the surface hydrodynamics of the Laptev Sea region. The cDOM is underestimated as C2R_a_gelbstoff. The strong absorption in the visible wavelength range that occurs due to the high cDOM concentrations is operationally attributed towards high Chl *a* concentration. The over-estimation of the order of one magnitude of Chl *a* occurs with all standard NASA and ESA processing algorithms because the standard assumption in all operational Ocean Colour algorithms contributes the main absorption towards the phytoplankton absorption. Also, the bio-optical measurements of the LENA2011 expedition in the organic-rich Lena River waters indicate that the regional specific phytoplankton absorption coefficient is around 3 times higher and more effective (Örek et al., 2013) than the value of a global mean. We propose that due to elevated cDOM background concentrations and the

very effective phytoplankton absorption all global ESA and NASA Chl *a* products show Chl *a* concentrations of one magnitude too high for the Siberian inner shelf regions (e.g. Fig. 6).

For an Ocean Colour investigation in the Kara Sea, Pozdnyakov et al. (2005) processed Ocean Colour MODIS time series from the ice-free season in 2003 combining the neural network and Levenberg-Marquardt multivariate processing. To obtain synoptic spatial distributions, temporally merged image mosaics based on calculated arithmetic means were generated. The authors compared the magnitude of MODIS calculated parameters of summer averages to ranges in the literature and showed that they had produced realistic DOC and SPM concentrations. Hessen et al. (2010) described match-ups of these Levenberg-Marquadt based processed MODIS products from summer 2003 with field-based data. While the range and distribution of DOC assessed from MODIS and in-situ sampling were in relative agreement with the deviation of the order of half a magnitude, the MODIS-derived Chl-concentrations were an order of magnitude too high. Hessen et al. (2010) assumed that the reason of the over-estimation is that in-situ sampling was performed in late-summer compared to the calculated MODIS summer average. However, as it is an outcome of this study, we assume that the Chl *a* overestimation by one order of magnitude described in Hessen et al. (2010) for the Ob Estuary in the southern Kara Sea is technically also due to the high background of cDOM ($> 5\,\mathrm{mg\,L^{-1}}$ DOC for the coastal Kara Sea waters).

A further confirmation gives Örek et al. (2013) undertaking bio-optical measurements at the LENA2011 expedition in early July 2011 to provide new field-based coefficients for a specified Ocean Colour processing for the Laptev Sea region. The authors discuss the difficulty of the calculation of Chl *a* from the water-leaving reflectances because phytoplankton absorption only contributed $< 10\,\%$ to the overall absorption that was dominated by absorption of the terrestrial organic.

5.2 Spatial hydrodynamical pattern of the Southern Laptev Sea

We did not observe a well-defined Lena River plume in the spatial distribution of C2R_a_gelbstoff and C2R_TSM or related turbidity parameters (C2R_k_{min}, C2r_Z90). However, multi-year expedition data show that the southern Laptev Sea is characterised by a wide-spread high freshwater signal and background cDOM concentrations (e.g. $a443_{cDOM}$ range in Buor Khaya Bay is 2 to 2.5 m^{-1}) and that the cDOM concentration of the Lena River in August is of the same magnitude as in the surface waters around the Lena River Delta and in Buor Khaya Bay in the August and September months. That the magnitude of concentrations is of the same order or higher in the coastal waters around the Lena River Delta and in Buor Khaya Bay then in the Lena River water is also a finding related to POC, nutrients (NO_3, PO_4) pCO_2 and oxygen saturation from multi-year expedition data (Semiletov et al., 2013). For the Laptev Sea region, Semiletov et al. (2013) show how high cDOM always correlated with low-salinity and how POC, nutrients and pCO_2 correlated with different ranges of salinity. The authors relate high cDOM to fluvial discharge and terrestrial POC and nutrients to coastal erosion. In summary, the high background DOC surrounding the Lena River Delta and in Buor Khaya Bay represents the wide-spread fresh water on the Laptev Sea shelf seem to be cover riverine DOC signals in the summer months of July, August and September.

Wegner et al. (2013) describe a SPM-enriched fresh water surface layer up to latitude of 76.8° N north of the Lena River Delta and 77.8° N on the eastern shelf due to dominating offshore winds, in September 2008, a non-normal year of anti-cyclonic atmospheric circulation pattern. Even in September 2007, in a quasi-normal year of cyclonic atmospheric circulation pattern, with dominating onshore winds and eastward, non cross-shelf transport of the riverine freshwater, Wegner et al. (2013) describe that SPM-enriched fresh water was measured up to latitude of 75° N. The authors showed that this contrasting fresh-water transport could also be made visible in the mapped MERIS C2R-parameters: in 2008, the outer shelf areas showed less transmissivity

(higher C2R_k_{min}, lower C2R_Z90) compared to more transparent waters on the outer shelf in 2007 (Wegner et al., 2013).

Due to obscuring continuous cloud coverage north of 75° N at a longitude of 130° E and westwards of it, the most transparent, lowest cDOM and SPM-water type is limited to be visible only within a few small cloud-free patches in the MERIS time series. Regularly, the high gradient between high-cDOM freshwater-influenced surface waters to low-cDOM marine-background waters seems to lie northwards of the cloud-free mapped areas under a continuous cloud coverage over the sea-ice free waters in summer. However, still under these limited conditions do the MERIS snapshots indicate that the spatial pattern of the transparent waters and the different types of less transparent waters do outline a coastal turbid meandering zone of several 100 km. Only in the year of prevailing anti-cyclonic atmospheric circulation in 2008, this week turbidity spatial pattern was partly hidden due to higher far-reaching diffuse turbidity of surface waters on the outer shelf.

The horizontal meander-fields and filament-fields in the Southern Laptev Sea suggest that a high frontal instability is continuously being generated. The frontal instability may be shed from the Lena River inflow and from unstable coastal currents. Meanders, filaments and eddies horizontally transport material in the surface water layer due to hydrodynamical equilibrium forces. Hydrodynamical model simulations and mooring current measurements show that these horizontal structures also provide vertical motion and indicate the vertical mixing of a surface layer (e.g. Chao and Shaw, 2002, Ralph 2002, Sutherland et al., 2011, Fong et al., 2002). Kraberg et al. (2013) show a well-mixed fresh-water influenced upper layer of 5 to 8 m depth in the Buor Khaya Bay. The rich hydrographic spatio-temporal pattern of filament-fields, meander-fields and eddies suggests that they carry chemical and biological fields and could trigger a high patchiness of phytoplankton and zooplankton in the Laptev See region. Kraberg et al. (2013) discuss a high spatial heterogeneity in phytoplankton composition in August 2010 in the Buor Khaya Bay.

The visualisation of resuspension events in the mapped MERIS C2R parameters highlights vertical mixing events down to the sea bottom of shallow banks in the southern Laptev Sea region. A turbidity belt around the Lena River delta is always visible. Reimnitz (2000) describes the high-latitudinal specific shallow bench around the Lena River Delta and other Arctic deltas that has been most probably generated by bottom-fast ice cover. Eicken et al. (2005) describe that the presence of the wide shallow bench around the Lena River Delta is in line with the mostly extensional sea-ice regime in this area.

Several shallow banks are delineated by the 5 m, 10 m and 15 m isobaths (State Geological Map of Russian Federation, 1999) on the Laptev Sea shelf and in the western part of the East Siberian Sea shelf. Gavrilov et al. (2003) discuss that the present-day shallow banks represent former Ice-Complex islands that have been destroyed by coastal thermal erosion and thermal abrasion during the last 1000 yr. Gavrilov et al. (2003) cite observations made on Russian seismic expeditions during the summer months that described the local turbidity on these shallow banks (in Lisitsin et al., 2000; Dmitrenko et al., 2001).

Charkin et al. (2011) discuss that for the shallow Laptev Sea, the impacted zone by resuspension events should be on average down to the 10 m bathymetry (with an estimation of average wave height of 1 m), accounting for the only short durability of strong waves. They describe how the dominating sand to sandy silt fraction that they found on the shallows and on the shallow bench around the Lena River Delta supports the theory of vertical mixing events that bring velocity currents down to these bathymetric depths. Vonk et al. (2012) confine a potential sedimentational regime to the shelf areas below 30 m depth, thereby excluding half of the shelf area of the Laptev Sea and Eastern Siberian shelf. Wegner et al. (2013) discuss that sediment entrainment due to resuspension at depths around 30 m take place mainly after storm events. Their data are based on current speeds of the ANABAR mooring station (74° 30′ N, 127° 20′ E) in the Laptev Sea. To further understand the processes of deposition of terrestrial material on the Laptev Sea and Eastern Siberian shelf regions the Ocean Colour remote

sensing may provide the information on hydrodynamic structures during the ice-free season. analyzing the resuspension events visible in the Ocean Colour satellite data may allow to spatially distinguish between the submarine depths of regular submarine seabed erosion and entrainment and the submarine depths where abrasion occurs only caused by strong storm events.

Ocean Colour remote sensing proves to provide new hydrodynamic information for the shallow Siberian inner shelf waters and coastal waters. The synoptic information on resuspension events, meandering and filamenting cannot be made visible from sampling from shipborne platforms because high-sea Arctic ship expeditions are forced to stay in deeper waters due to the draft of the ocean-going ships. Even with grid sampling from shallow-water going ships it would be difficult to capture these spatial features as sampling cannot logistically be done on a small enough spatial frequency. Deployment of drifting sensors could provide in future measurements on fronts, meanders, eddies, and filaments and support the validation of the remote sensing derived information.

The known main aquatic sediment transport during the ice-free seasons is regulated as a submarine sediment transport within the bottom nepheloid layer inside North–South running submarine valley structures that serve as transport pipes (Wegner et al., 2003, 2005). This submarine transport mechanism escapes the detection possibilities based on optical satellite data. However, the meanders, eddies and filaments also visualize a wide-spread lateral surface water transport of dissolved and particulate matter in the sea-ice free season. On the other hand, the hydrodynamical structures and resuspension zones also potentially indicate local blockades of cross-shelf horizontal transport and wide-spread processes for vertical transport pathways of nutrients, carbon, sediments and heat to the submarine sea bottom of at least 10 m depth.

6 Conclusions

Despite limitation due to high cloud coverage during the sea-ice free season, Ocean Colour remote sensing provides highly useful time-resolved information on the hydrographic dynamics of the shallow Siberian shelf regions.

During the ice-free season, the Lena River flows out in coastal and onshore waters of similar or even higher concentrations of SPM and cDOM. For SPM this is due to resuspension events of the shallow bench around the Lena River delta and on the numerous shallows of the shallow Laptev Sea bathymetry. The expedition data show that high cDOM concentrations are distributed all over in Buor Khaya Bay and in the coastal and inner shelf waters northeast of the Lena River Delta. Care must be taken in terms of Ocean-Colour derived Chl *a* concentrations that are highly overestimated by the order of one magnitude due to the elevated cDOM concentrations in coastal waters and the inner shelf surface waters.

Known lateral transport pathways in the Laptev Sea do function by transport within and on the sea-ice (Eicken et al., 1997, 2000) and submarine via the bottom nepheolid layer (Wegner et al., 2003, 2005). In addition, the spatio-temporal patterns of the Ocean Colour parameters indicate the lateral advection of terrestrial (dissolved and fine particulates) and living biological material during the ice-free season. Large meander crests, filaments and eddy-like structures is a critical point because the water masses carried inside these features will be less intensively horizontally mixed for longer periods of time during lateral advection processes.

This is an important result as it also explains the high heterogeneity of coastal phytoplankton and zooplankton communities. Furthermore it indicates potential vertical pathways for downward and upward transport of material. Resuspension events that were made visible in the Ocean Colour parameters show that the shallow regions, specifically the shallow bench around the Lena River, but also the wide-spread submarine shallows are regularly influenced by resuspension that indicates vertical mixing and vertical transport pathways of nutrients, carbon, sediments and heat.

Acknowledgements. This work is supported by the German Science Foundation (DFG 4575) and the Helmholtz Climate Initiative REKLIM (Regionale Klimaaenderungen/Regional climate change). The Russian–German LENA08, and LENA10 ship expeditions are supported and organized by the AWI (Germany) and the Arctic and Antarctic Research Institute, AARI (St.-Petersburg, RU). The vessels used were the Russian river vessel Puteyski 405 in 2008 and 2010, and PTS TB-0012 in Buor Khaya Bay in 2010. The TRANSDRIFT expedition is an integral part of the joined Russian–German project "Laptev Sea System". It is funded by the German Federal Ministry for Education and Research and the Russian Ministry of Education and Science. The vessel used for the TRANSDRIFT-XVII expedition in September 2010 was the RV NIKOLAY EVGENOV. We thank the captains and the crews for their support.

We thank Ruth Flerus, AWI/GEOMAR, who sampled and prepared the cDOM samples at the LENA2010 ship expedition and the OSL, St.-Petersburg (RU), specifically Elena Dobrotina, for the support for the cDOM-measurements of all expeditions. We thank Bennet Juhls, University of Kiel/GEOMAR, for the NCEP wind analyses.

The ESA ENVISAT project (MERIS-ID 5504) granted the used MERIS data. The ESA ENVISAT project (MERIS-ID 5504) granted the used MERIS data. We thank the German Aerospace Agency (DLR) for providing RapidEye data by the RESA (RapidEye Science Archive) program (grant number 424 Geomonitoring PROGRESS).

References

Aagaard, K. and Armack, E.: The role of sea ice and other fresh water in the Arctic circulation, J. Geophys. Res., 94, 14485–14489, 1989.

Bauch, D., Dmitrenko, I. A., Wegner, C., Hölemann, J. A., Kirillov, S. A., Timokhov, L. A., and Kassens, H.: Exchange of Laptev Sea and Arctic Ocean halocline waters in response to atmospheric forcing, J. Geophys. Res., 114, C05008, 2156–2202, 2009.

Chao, S.-Y. and Shaw, P. T.: Nonhydrostatic aspects of coastal upwelling meanders and filaments off eastern ocean boundaries, Tellus A, 54, 63–75, 2002.

Charkin, A. N., Dudarev, O. V., Semiletov, I. P., Kruhmalev, A. V., Vonk, J. E., Sánchez-García, L., Karlsson, E., and Gustafsson, Ö.: Seasonal and interannual variability of sedimentation and organic matter distribution in the Buor-Khaya Gulf: the primary recipient of

input from Lena River and coastal erosion in the southeast Laptev Sea, Biogeosciences, 8, 2581–2594, doi:10.5194/bg-8-2581-2011, 2011.
Dmitrenko, I. A., Hoelemann, J., Kirillov, S. A., Wegner, C., Gribanov, V. A., Berezovskaya, S. L., and Kassens, H. M.: Thermal regime of the bottom water layer in the Laptev Sea and determining processes, Kriosfera Zemli, 5, 40–55, 2001 (in Russian).
Doerffer, R. and Schiller, H.: The MERIS case 2 water algorithm, Int. J. Remote Sens., 28, 3–4, 517–535, 2007.
Doerffer, R. and Schiller, H.: MERIS Regional Coastal and Lake Case 2 Water Project Atmospheric Correction, GKSS-KOF-MERIS-ATBD01, Institute for Coastal Research, GKSS Research Center, Geesthacht, 42 pp., 2008.
Eicken, H., Reimnitz, E., Alexandrov, V., Martin, T., Kassens, H., and Viehoff, T.: Sea-ice processes in the Laptev Sea and their importance for sediment export, Cont. Shelf Res., 17, 205–233, 1997.
Eicken, H., Kolatschek, J., Freitag, J., Lindemann, F., Kassens, H., and Dmitrenko, I.: Identifying a major source area and constraints on entrainment for basin-scale sediment transport by Arctic sea ice, Geophys. Res. Lett., 27, 1919–1922, 2000.
Eicken, H., Dmitrenko, I., Tyshko, K., Darovskikh, A., Dierking, W., Blahak, U., Groves, J., and Kassens, H.: Zonation of the Laptev Sea landfast ice cover and its importance in a frozen estuary, Global Planet. Change, 48, 55–83, 2005.
Fong, D. A. and Geyer, W. R.: The alongshore transport of freshwater in a surface-trapped river plume, J. Phys. Oceanogr., 32, 957–972, 2002.
Gavrilov, A. V., Romanovskii, N. N., Romanovsky, V. E., Hubberten, H.-W., and Tumskoy, V. E.: Reconstruction of ice complex remnants on the Eastern Siberian Arctic shelf, Permafrost Periglac., 14, 187–198, 2003.
Gordeev, V. V., Martin, J.-M., Sidorov, I. S., and Sidorova, M. N.: A reassessment of the Eurasian river input of water, sediment, major elements and nutrients to the Arctic Ocean, Am. J. Sci., 296, 664–691, 1996.
Gustafsson, Ö., van Dongen, B. E., Vonk, J. E., Dudarev, O. V., and Semiletov, I. P.: Widespread release of old carbon across the Siberian Arctic echoed by its large rivers, Biogeosciences, 8, 1737–1743, doi:10.5194/bg-8-1737-2011, 2011.
Hessen, D. O., Carroll, J. L., Kjeldstad, B., Korosov, A. A., Pettersson, L. H., Pozdnyakov, D., and Sørensen, K.: Input of organic carbon as determinant of nutrient fluxes, light climate and productivity in the Ob and Yenisey estuaries, Estuar. Coast. Shelf Sci., 88, 53–66, 2010.

Holmes, R. M., McClelland J. W., Peterson, B. J., Tank, S. E., Bulygina, E., Eglinton, T. I., Gordeev, V. V., Gurtovaya, T. Y., Raymond, P. A., Repeta, D. J., Staples, R., Striegl, R. G., Zhulidov, A. V., and Zimov, S. A.: Seasonal and annual fluxes of nutrients and organic matter from large rivers to the Arctic Ocean and surrounding seas, Estuar. Coast., 35, 369–382, 2012.
International Ocean Colour Coordinating Group (IOCCG): Remote Sensing of Ocean Colour in Coastal, and Other Optically-Complex Waters, edited by: Sathyendranath, S., Reports of the International Ocean-Colour Coordinating Group, 3, IOCCG, Dartmouth, Canada, 2000.
Karlsson, E. S., Charkin, A., Dudarev, O., Semiletov, I., Vonk, J. E., Sánchez-García, L., Andersson, A., and Gustafsson, Ö.: Carbon isotopes and lipid biomarker investigation of sources, transport and degradation of terrestrial organic matter in the Buor-Khaya Bay, SE Laptev Sea, Biogeosciences, 8, 1865–1879, doi:10.5194/bg-8-1865-2011, 2011.
Kassens, H., Hölemann, J., Klagge, T., and Novikhin, A.: Russian–German Cooperation Laptev Sea: Expeditions TRANSDRIFT XII, XIV, XVI, Summer 2007, 2008, 2009, 2010, unpubl. cruise reports, 2010.
Kraberg, A. C., Druzhkova, E., Heim, B., Loeder, M. J. G., and Wiltshire, K. H.: Phytoplankton community structure in the Lena Delta (Siberia, Russia) in relation to hydrography, Biogeosciences Discuss., 10, 2305–2344, doi:10.5194/bgd-10-2305-2013, 2013.
Lantuit, H., Atkinson, D., Overduin, P. P., Grigoriev, M., Rachold, V., Grosse, G., and Hubberten, H.-W.: Coastal erosion dynamics on the permafrost-dominated Bykovsky Peninsula, north Siberia, 1951–2006, Polar Res., 30, 7341, doi:10.3402/polar.v30i0.7341, 2011.
Lantuit, H., Overduin, P. P., Couture, N., Wetterich, S., Are, F., Atkinson, D., Brown, J., Cherkashov, G., Drozdov, D., Forbes, D., Graves-Gaylord, A., Grigoriev, M., Hubberten, H. W., Jordan, J., Jorgenson, T., Ødegård, R. S., Ogorodov, S., Pollard, W., Rachold, V., Sedenko, S., Solomon, S., Steenhuisen, F., Streletskaya, I., and Vasiliev, A.: The Arctic Coastal Dynamics database, a new classification scheme and statistics on arctic permafrost coastlines, Estuar. Coast., 35, 383–400, 2012.
Lee, Z. P. and Hu, C. M.: Global distribution of Case-1 waters: an analysis from SeaWiFS measurements, Remote Sens. Environ., 101, 270–276, 2006.
Lisitsin, A. P., Shevchenko, V. P., and Burenkov, V. I.: Hydrooptics and suspended matter of Arctic seas, Atmos. Ocean. Opt., 13, 61–71, 2000.

Lobbes, J. M., Fitznar, H. P., and Kattner, G.: Biogeochemical characteristics of dissolved and particulate organic matter in Russian rivers entering the Arctic Ocean, Geochim. Cosmochim. Acta, 64, 2973–2983, 2000.

Loginova, A.N: Chromophoric dissolved organic matter in the Laptev Sea (Siberian Arctic): a comparison of in-situ observations, laboratory measurements, and remote sensing, MSc thesis "Applied Polar and Marine Sciences", POMOR, St. Petersburg State University (RU), and University of Hamburg (DE), 98 pp., 2011.

Morel, A. and Prieur, L.: Analysis of variations in ocean color, Limnol. Oceanogr., 22, 709–722, 1977.

Örek, H., Doerffer, R., Röttgers, R., Boersma, M., and Wiltshire, K. H.: A Bio-optical model for remote sensing of Lena water, submitted to Biogeosciences, 2013.

Pozdnyakov, D. V., Korosov, A. A., Pettersson, L. H., and Johannessen, O. M.: MODIS evidences the river run-off impact on the Kara Sea trophy, Int. J. Remote Sens., 26, 364–368, 2005.

Rachold, V., Grigoriev, M. N., Are, F. E., Solomon, S., Reimnits, E., Kassens, H., and Antonov, M.: Coastal erosion vs riverine sediment discharge in the Arctic Shelf seas, Int. J. Earth Sci., 89, 450–460, 2000.

Rachold, V., Eicken, H., Gordeev, V. V., Grigoriev, M. N., Hubberten, H.-W., Lisitzin, A. P., Shevchenko, V. P., and Schirrmeister, L.: Modern terrigenous organic carbon input to the Arctic Ocean, in: Organic Carbon Cycle in the Arctic Ocean: Present and Past, edited by: Stein, R. and Macdonald, R. W., 33–55, 2004.

Reimnitz, E.: Interactions of river discharge with sea ice in proximity of Arctic Deltas: a review, Polarforschung, 70, 123–134, 2000.

Schirrmeister, L., Siegert, C., Kunitzky, V. V., Grootes, P., and Erlenkeuser, H.: Late quaternary ice rich permafrost sequences as a palaeoenvironmental archive for the Laptev Sea region in northern Siberia, Int. J. Earth Sci., 91, 154–167, 2002.

Scott, P., Zaneveld, J. R. V., Mitchell, B. G., Mueller, J. L., Kahru, M., Wieland, J., and Stramska, M.: Inherent optical properties: instruments, characterizations, field measurements and data analysis protocols, in: Ocean Optics Protocols For Satellite Ocean Color Sensor Validation, vol. IV, edited by: Mueller, J. L., Fargion, G. S., and McClain C. R., NASA/TM-2003-211621/Rev4, 4, 76 pp., 2000.

Semiletov, I. P., Pipko, I. I., Shakhova, N. E., Dudarev, O. V., Pugach, S. P., Charkin, A. N., McRoy, C. P., Kosmach, D., and Gustafsson, Ö.: Carbon transport by the Lena River from

its headwaters to the Arctic Ocean, with emphasis on fluvial input of terrestrial particulate organic carbon vs. carbon transport by coastal erosion, Biogeosciences, 8, 2407–2426, doi:10.5194/bg-8-2407-2011, 2011.

Semiletov, I. P., Shakhova, N. E., Pipko, I. I., Pugach, S. P., Charkin, A. N., Dudarev, O. V., Kosmach, D. A., and Nishino, S.: Space-time dynamics of carbon stocks and environmental parameters related to carbon dioxide emissions in the Buor-Khaya Bay of the Laptev Sea, Biogeosciences Discuss., 10, 2159–2204, doi:10.5194/bgd-10-2159-2013, 2013.

Stern, M. E., Chassignet, E. P., and Whitehead, J. A.: The wall jet in a rotating fluid, J. Fluid Mech., 335, 1–28, 1997.

Sutherland, D. A., Straneo, F., Lentz, S., and St-Laurent, P.: Observations of fresh, anticyclonic eddies in the Hudson Strait outflow, J. Mar. Syst., 88, 375–384, 2011.

Vonk, J. E., Sánchez-García, L., Semiletov, I., Dudarev, O., Eglinton, T., Andersson, A., and Gustafsson, Ö.: Molecular and radiocarbon constraints on sources and degradation of terrestrial organic carbon along the Kolyma paleoriver transect, East Siberian Sea, Biogeosciences, 7, 3153–3166, doi:10.5194/bg-7-3153-2010, 2010.

Vonk, J. E., Sánchez-García, L., van Dongen, B. E., Alling, V., Kosmach, D., Charkin, A., Semiletov, I. P., Dudarev, O. V., Shakhova, N., Roos, P., Eglinton, T., Andersson, A., and Gustafsson, O.: Activation of old carbon by erosion of coastal and subsea permafrost in Arctic Siberia, Nature, 489, 137–140, 2012.

Wagner, D., Overduin, P. P., Grigoriev, M. N., Knoblauch, C., and Bolshiyanov, D. Y.: Russian–German cooperation System Laptev Sea: the expedition LENA 2008, Berichte zur Polar- und Meeresforschung, Alfred Wegener Institute for Polar and Marine Research, Bremerhaven, 642, 132 pp., 2012.

Wegner, C., Hölemann, J. A., Dmitrenko, I., Kirillov, S. A., Tuschling, K., Abramova, E., and Kassens, H.: Suspended particulate matter on the Laptev Sea shelf (Siberian Arctic) during ice-free conditions, Estuar. Coast. Shelf Sci., 57, 55–64, 2003.

Wegner, C., Hölemann J. A., Dmitrenko, I., Kirillov, S. A., and Kassens, H.: Seasonal variations in sediment dynamics on the Laptev Sea shelf (Siberian Arctic), Global Planet. Change, 48, 126–140, 2005.

Wegner, C., Bauch, D., Hölemann, J. A., Janout, M. A., Heim, B., Novikhin, A., Kirillov, S., Kassens, H., and Timokhov, L.: Interannual variability of surface and bottom sediment transport on the Laptev Sea shelf during summer, Biogeosciences Discuss., 9, 13053–13084, doi:10.5194/bgd-9-13053-2012, 2012.

Table 1a. LENA2010, July to August 2010: data used in this study.

Station	Codes	Date	Match-up data
1	T1-10-02; L10-21	29 Jul & 4 Aug 2010	transmissivity, cDOM (4 Aug 2010)
2	T1-10-01; L10-23	29 Jul & 4 Aug 2010	transmissivity, cDOM (4 Aug 2010)
4	T1-10-04; L10-24	29 Jul & 4 Aug 2010	transmissivity, cDOM (4 Aug 2010)
5	T1-10-05; L10-25	30 Jul & 4 Aug 2010	transmissivity, cDOM (4 Aug 2010)
9	T2-10-02; L10-28	31 Jul & 5 Aug 2010	transmissivity, cDOM (5 Aug 2010)
11	T2-10-04; L10-31	31 Jul & 5 Aug 2010	transmissivity, cDOM (5 Aug 2010)
26	L10-36	6 Aug 2010	transmissivity, cDOM (6 Aug 2010)

Table 1b. TRANSDRIFT-XVII, September 2010: data used in this study.

Station	Code	Date	Match-up data
1	NE10-01	9 Sep 2010	cDOM, SPM, Chl
2	NE10-02	9 Sep 2010	cDOM, SPM, Chl
3	NE10-03	9 Sep 2010	cDOM, SPM, Chl
4	NE10-04	9 Sep 2010	SPM, Chl
5	NE10-05	9 Sep 2010	cDOM, SPM, Chl
6	NE10-06	10 Sep 2010	cDOM, SPM, Chl
8	NE10-08	12 Sep 2010	cDOM, SPM, Chl
9	NE10-09	12 Sep 2010	cDOM, SPM, Chl
10	NE10-10	12 Sep 2010	cDOM, SPM, Chl
13	NE10-13	12 Sep 2010	SPM, Chl
14	NE10-14	13 Sep 2010	SPM, Chl
15	NE10-15	13 Sep 2010	SPM, Chl
16	NE10-16	13 Sep 2010	cDOM, SPM, Chl
17	NE10-17	13 Sep 2010	cDOM, SPM, Chl
19	NE10-19	13 Sep 2010	cDOM, SPM, Chl
20	NE10-20	16 Sep 2010	cDOM, SPM, Chl
21	NE10-21	16 Sep 2010	cDOM, SPM, Chl
22	NE10-22	16 Sep 2010	cDOM, SPM, Chl
23	NE10-23	16 Sep 2010	cDOM, SPM, Chl
27	NE10-27	17 Sep 2010	cDOM, SPM, Chl
28	NE10-28	17 Sep 2010	cDOM, SPM, Chl
29	NE10-29	18 Sep 2010	cDOM, SPM, Chl
30	NE10-30	18 Sep 2010	cDOM, SPM, Chl
34	NE10-34	18 Sep 2010	cDOM, SPM, Chl
35	NE10-35	19 Sep 2010	cDOM, Chl

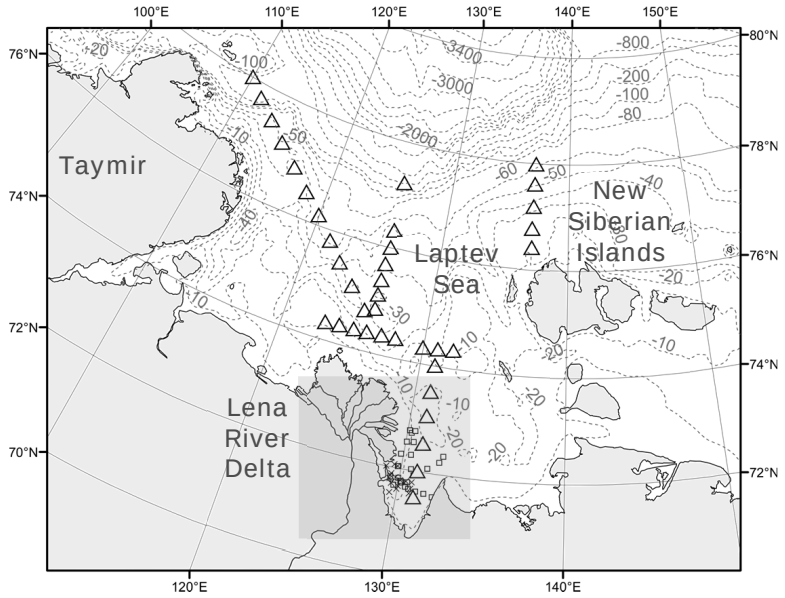

Fig. 1a. The southern Laptev Sea, Arctic Siberia (RU). Stations of the TRANSDRIFT-XVII ship expedition (from 9 to 20 September 2010) from the inner shelf to the outer shelf waters of the Laptev Sea are displayed as triangles. Stations of the LENA2008 ship expedition south-east of the Lena River Delta (from 9 to 14 August 2008) are small symbols displayed as crosses. Stations of the LENA2010 ship expedition in the Buor-Khaya Bay (from 29 July to 7 August 2010) are small symbols displayed as squares.

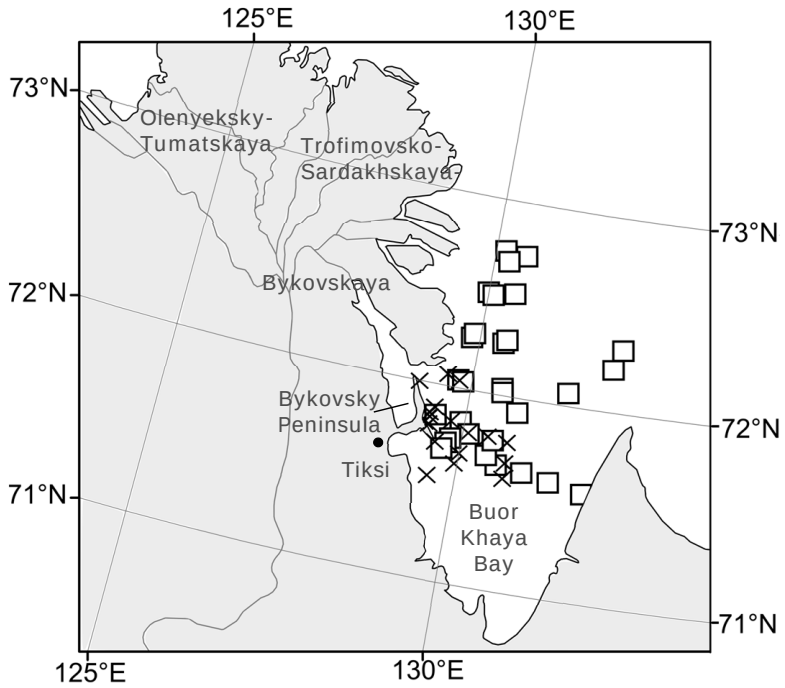

Fig. 1b. Buor Khay Bay, southeastern Laptev Sea, Arctic Siberia (RU). South-East of the Bykovskaya river branch of the Lena River, the Bykovsky Peninsula shelters the Tiksi Bay. Stations of the LENA2008 ship expedition south-east of the Lena River Delta (from 9 to 14 August 2008) are displayed as crosses. Stations of the LENA2010 ship expedition in the Buor-Khaya Bay (from 29 July to 7 August 2010) are displayed as squares.

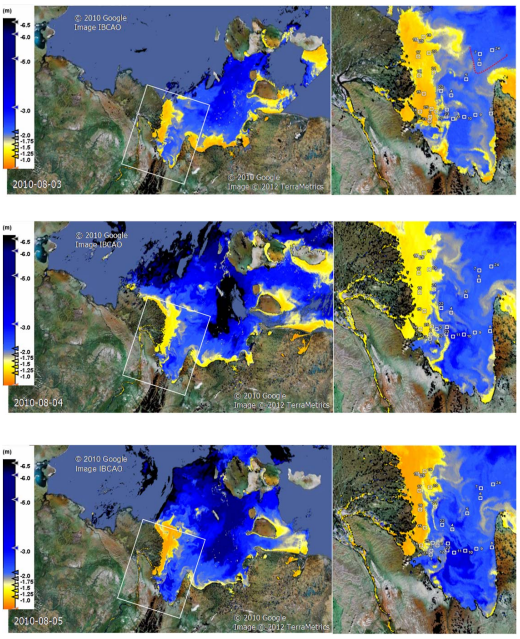

Fig. 2. MERIS colour-coded maps on 3, 4 and 5 August 2010 of the calculated C2R parameter C2R_Z90, the first attenuation depth, with zoom to the LENA2010 stations (squares) east of the Lena River Delta, Buor Khaya Bay within the time window of the LENA2010 ship expedition (from 29 July to 7 August 2010). The salinity isoline = 8 PSU derived from the LENA210 ship expedition is schematically displayed as red outline close to the most north-eastern LENA2010 stations 6, 7, 24. Southwards, the freshwater dominates the surface waters with a salinity of < 5.

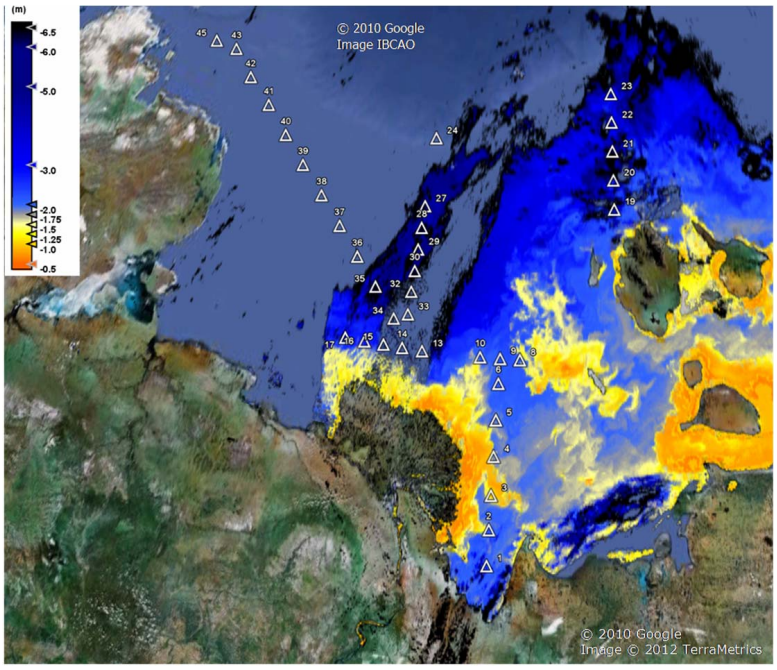

Fig. 3. MERIS colour-coded map of C2R_Z90, the first attenuation depth, 7 September 2010 at 10:48 (local time). Stations of the TRANSDRIFT-XVII ship expedition in September 2010 are displayed as triangles.

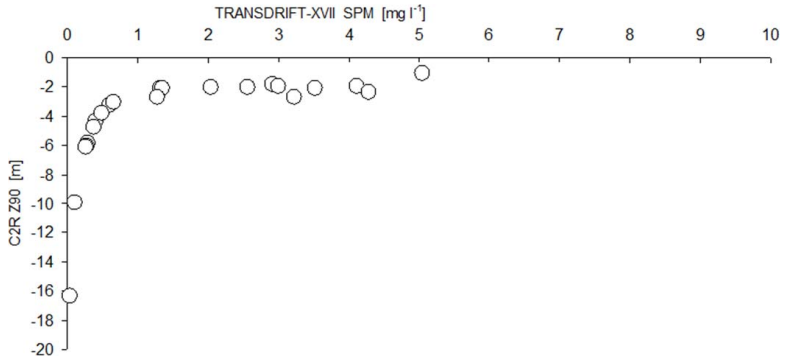

Fig. 4a. TRANSDRIFT-XVII SPM (from 9 to 20 September 2010) vs. MERIS C2R_Z90 calculated from the MERIS acquisition on 7 September 2010, $n = 21$.

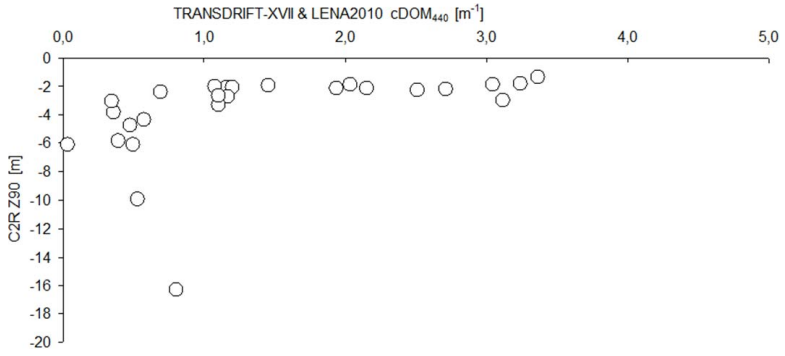

Fig. 4b. TRANSDRIFT-XVII & LENA2010 $cDOM_{440}$ vs. MERIS C2R-Z90. LENA2010: C2R_Z90 was taken from the most MERIS concomitant acquisitions closest in time to the sampling: 3, 4, 6 August 2010 and was matched with LENA2010 $cDOM_{440}$, respectively, $n = 7$. TRANSDRIFT-XVII: C2R_Z90 was taken from 7 September 2010, and matched with $cDOM_{440}$ (9 to 12 September 2010) using all available pixels within relatively homogenous environments, but of satellite acquisition 2 to 5 days later, $n = 22$.

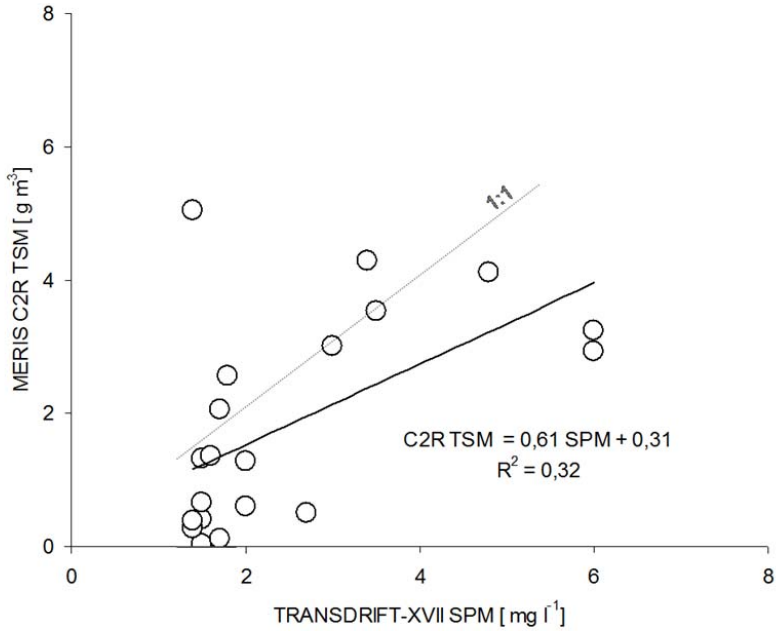

Fig. 5. TRANSDRIFT-XVII SPM (from 9 to 20 September 2010) vs. MERIS C2R_TSM calculated from the MERIS acquisition on 7 September 2010, $n = 21$.

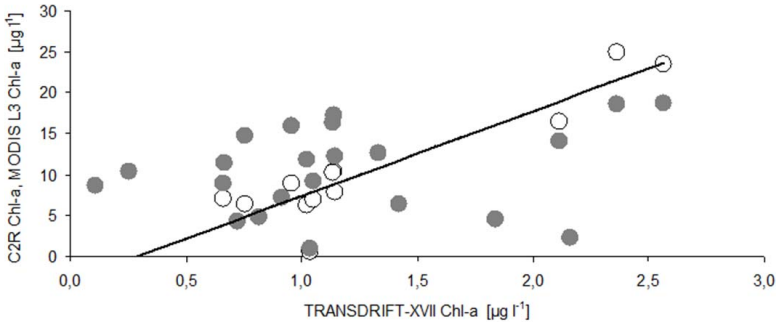

Fig. 6. TRANSDRIFT-XVII Chl *a* (9 to 20 September 2010) vs. MERIS C2R_Chl *a* (7 September 2010) displayed as filled circles, $n = 23$. TRANSDRIFT-XVII Chl *a* (9 to 20 September 2010) vs. MODIS Level3 Chl *a* (averaged Chl *a* concentration in September 2010, 9 km spatial resolution), displayed as white circles, $n = 11$. Both remote sensing Chl *a* products are overestimated by the order of one magnitude.

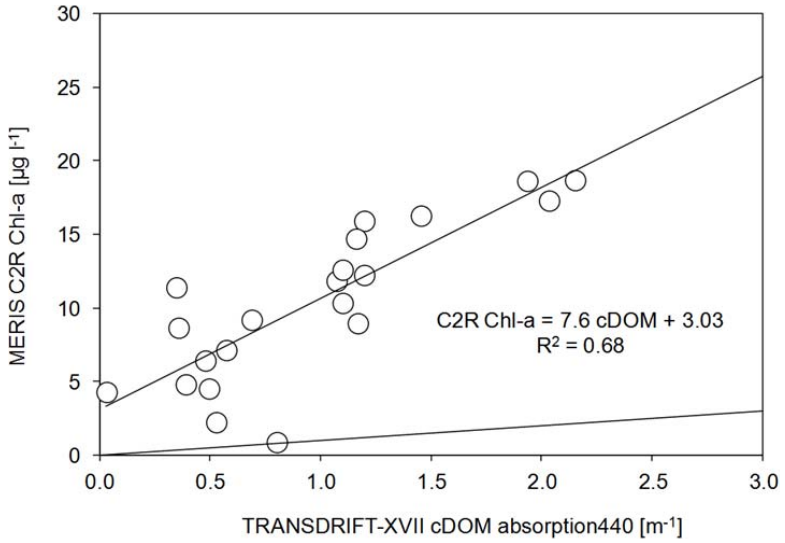

Fig. 7. TRANSDRIFT-XVII acDOM440 (from 9 to 20 September 2010) vs. MERIS C2R_Chl *a* calculated from the MERIS acquisition on 7 September 2010, $n = 23$.

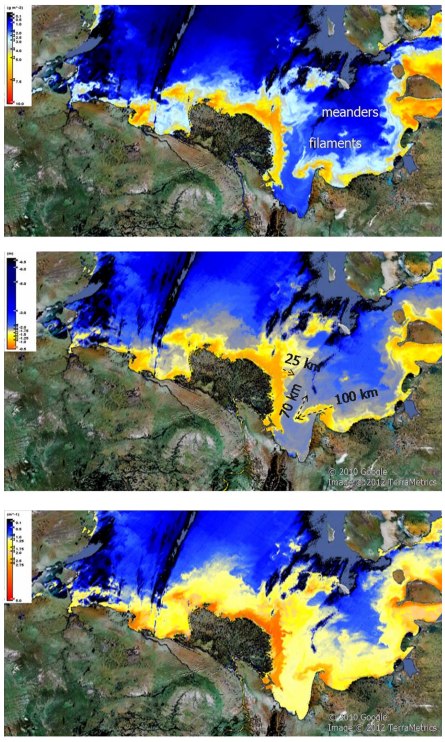

Fig. 8. (a–c) MERIS colour-coded maps of the Southern Laptev Sea, on 25 September 2009, at 11:55 (local time) visualise the fields of meanders and filaments. The mapped C2R parameters are **(a)** MERIS C2R_TSM ($g m^{-3}$), **(b)** MERIS C2R_Z90 (m), **(c)** MERIS C2R_absorption (m^{-1}).

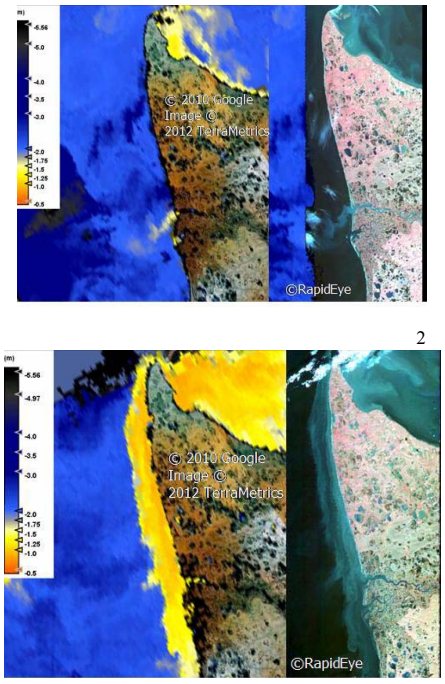

Fig. 9. (a) RapidEye False-Colour NIR-Composite (TOA-radiances) (8 August 2010) and the mapped MERIS parameter C2R_Z90 (m^{-1}) (8 August 2010) visualize transparent waters along the eastern Buor Khaya Bay coast and a spatially confined turbid river inflow into Buor Khaya Bay. **(b)** RapidEye False-Colour NIR-Composite (TOA-radiances) (27 August 2010) and the mapped MERIS parameter C2R_Z90 (m^{-1}) (27 August 2010) after storm events (http://www.ncep.noaa.gov/) in August 2010 visualize the turbidity zone along the eastern Buor Khaya Bay coast above the shallow submarine slope.